Gold Nanoparticle Catalysis of the *Cis-Trans* Isomerization of Azobenzene

Geniece L. Hallett-Tapley,[a] Claudio D'Alfonso,[a,b] Natalia L. Pacioni,[a,c] Christopher D. McTiernan,[a] María González-Béjar,[a,d] Osvaldo Lanzalunga,[b] Emilio I. Alarcon,[a] and Juan C. Scaiano [a,d]*

[a] *Department of Chemistry and Centre for Catalysis Research and Innovation, University of Ottawa, 10 Marie Curie, Ottawa K1N 6N5, Canada*

[b] *Dipartimento di Chimica, Sapienza Università di Roma and Istituto CNR di Metodologie Chimiche (IMC-CNR), Sezione Meccanismi di Reazione, P.le A. Moro 5, 00185 Rome, Italy*

[c] *Current address: Departamento de Química, INFIQC, Facultad de Ciencias Químicas, Universidad Nacional de Córdoba, Ciudad Universitaria, 5000 Córdoba, Argentina*

[d] *Current address: Instituto de Ciencia Molecular/ Departamento de Química Orgánica, Universidad* de Valencia, C/ Catedrático José Beltrán, 2, 46980, Paterna, Valencia, Spain

*Author to whom correspondence should be addressed.
Email: scaiano@photo.chem.uottawa.ca

Table of Contents

Experimental.

Materials. *trans*-Azobenzene, *trans*-4-methoxyazobenzene, *trans*-4,4'-dichloroazobenzene, 4,4'-dimethylazobenezne, gold (III) tetrachloroauric acid hydrate ($HAuCl_4•3H_2O$), 50% H_2O_2, manganese dioxide (MnO_2) and HPLC grade CH_3CN were all purchased from Sigma Aldrich and used as received. All reactions were carried out using MilliQ deionized, distilled water (resistivity 18.2 MΩ cm^{-1} at 25°C; 0.22 μm filter).

Synthesis of Gold Nanoparticles. Gold nanoparticles were prepared using a previously described technique where H_2O_2 was employed as the reducing agent.[S1] AuNP were ablated using laser excitation from a 532 nm Continuum Nd/YAG laser (~8 ns/pulse) with an overall power of 45 mJ/shot. The term "pseudo-naked" nanoparticles refers to AuNP where no additional organic stabilizer is added to the mixture. To allow for sufficient ripening, AuNP were allowed to stand, in the dark, overnight. Excess H_2O_2 was removed from the AuNP colloid by treatment of 5 mL ablated AuNP with 40-50 mg of MnO_2 for 5 minutes, during which time considerable gas evolution was observed as a result of excess peroxide decomposition. The suspension was vacuum filtered through a 0.22 μm cellulose acetate filter to remove any traces of MnO_2 (purchased from Fisher Scientific) from the mixture. Removal of excess H_2O_2 was confirmed *via* HPLC analysis where H_2O_2 was identified by a peak at retention time 4.5 min (Waters Integrity HPLC, reverse phase C18 Zorbax column, 60:40 CH_3CN/MilliQ H_2O eluent mixture, 0.5 mL/min flow rate). Importantly, a consistent laser power and beam homogeneity have been found to be integral in the formation of stable, pseudo-naked AuNP for use in this work.

After 3 days, minimal aggregation of the treated, ablated AuNP was detected, observed as broadening of the absorption spectrum at $\lambda_{max} \approx 600$ nm. Following 1 week, the NP exhibited considerable aggregation and changed color from a deep pink to slightly purple (Figure S4a). As such, AuNP were used immediately following filtration. As the characteristics of the AuNP can vary from batch to batch, all comparative experiments (*i.e.,* substituent effects or concentration studies) were carried out using the same batch of nanoparticles to ensure for accurate comparison between results. The approximate concentration and size of naked AuNP synthesized using this methodology has been calculated as being ~ 6 nM and 12 ± 2.5 nm, respectively.[S2]

AuNP catalyzed *cis-trans* azobenzene isomerization. A Cary 50 spectrophotometer in scanning kinetics mode was used to monitor all isomerization experiments. All experiments were carried out in duplicate, with the average rate constants of the two trials being presented. For a typical experiment, the commercially available *trans* isomers were photochemically converted to the *cis* derivative using the following procedure. 1 mL of a 10 mM solution of the *trans*-azobenzenes in HPLC grade CH_3CN were irradiated in a glass NMR tube using 14 UVA lamps in a Luzchem photoreactor for 30 minutes. After the allotted time, UV-visible spectroscopy was used to confirm complete conversion of the *trans* to the *cis* isomer (Figure S1). The samples were stored in brown vials, in the dark and fridge, to prevent any residual thermal conversion back to the *trans* form. For a typically spectroscopic measurement, 100 μL of ablated AuNP (192 pM) were added to 3 mL of water in a 1 cm × 1 cm quartz cuvette containing 15 μL (48 μM) of the original 10 mM azobenzene stock solutions in CH_3CN. It should be noted that the 4,4'-dichloroazobenzene was somewhat less soluble in CH_3CN than the other two derivatives studied in this work, thus 30 μL of stock solution was added to ensure that all trials were started with an initial absorption of the π- π* transition of the azobenzene of between abs ≈ 0.2 – 0.4 ($\lambda_{max}{}^{cis}$ = 295 nm (**1**), 310 nm (**2**), 300 nm (**3**), 300 nm (**4**)).

The growth of the *trans*-azobenzenes formed in the presence of ablated AuNP was monitored at the maximum wavelength of absorption for each *trans* stereoisomer and collected as a function of time. All isomer growths proceeded in a first-order manner and the kinetic data was fitted to a simple, first-order rate law (eq. 1) using Kaleidagraph graphing software.

$$A_t = A_\infty + (A_o - A_\infty)e^{-kt} \tag{1}$$

In this equation, A_t is the absorption of the *trans* isomer at time t, A_o is the initial absorption of at λ_{max} of the *trans* isomer after addition of AuNP, A_∞ is the maximum absorption obtained in the plateau region of the growth curve and k is the observed first-order rate constant.

Determination of Conversion Rate (Figure S5). Prior to any form of data analysis, the raw absorbance *vs*. time data was corrected to remove any residual contributions of the *cis*-isomer from the absorption spectra, effectively allowing for the initial concentration of the *trans*-stereoisomer at time 0 to zero.

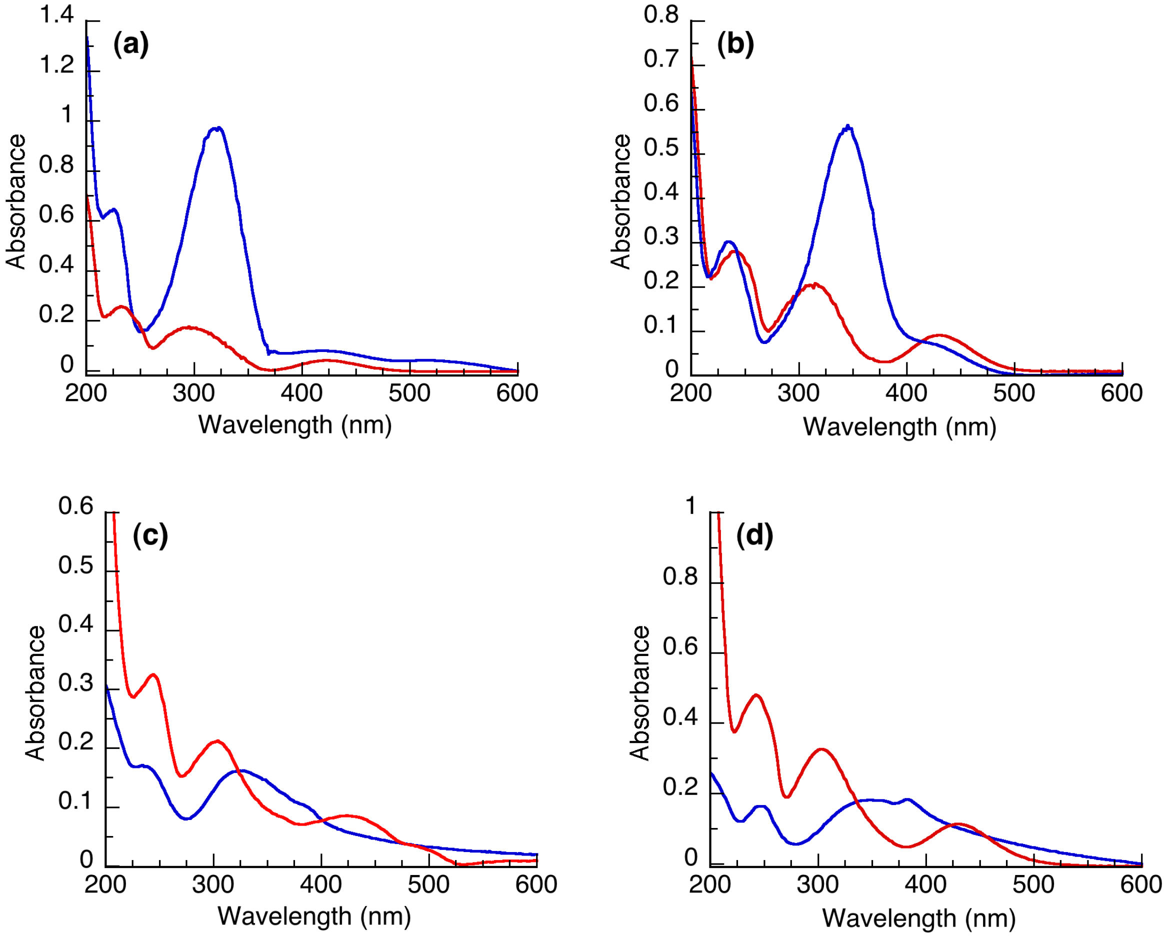

Figure S1. UV-visible spectra of *trans* (blue) and *cis* (red) photoisomerization of (a) azobenzene **1**, (b) 4-methoxyazobenzene **2**, (c) 4,4'-dichloroazobenzene **3,** and (d) 4,4'-dimethylazobenzene **4** following 30 minutes of UVA irradiation.

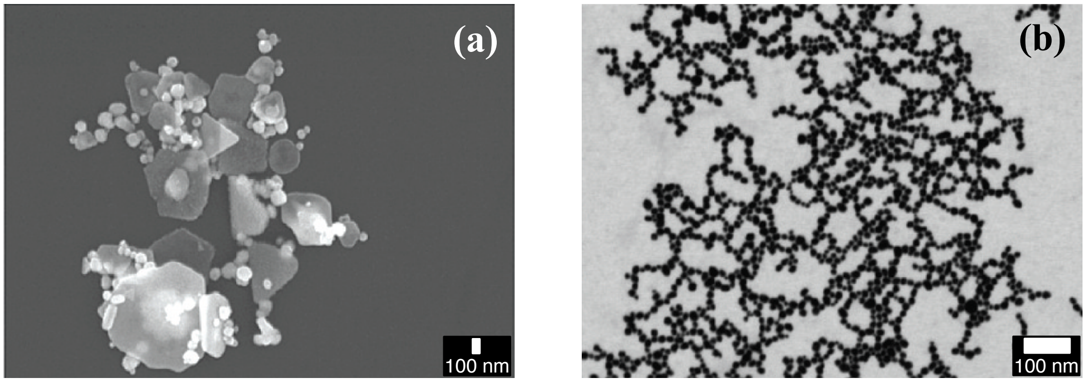

Figure S2. SEM images taken of H_2O_2-generated AuNP (a) before and (b) after ablation. Reproduced from reference S2.

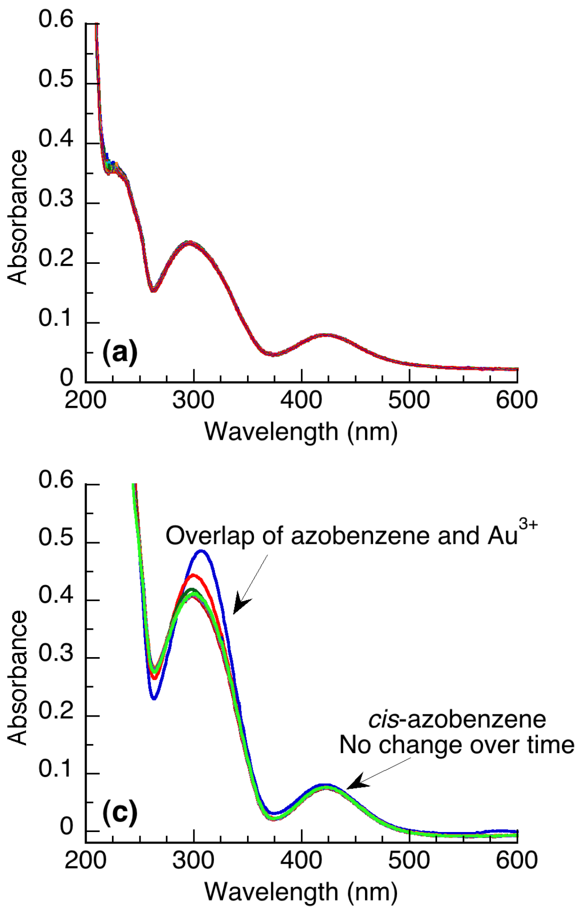

Figure S3. Control experiments for thermal *cis-trans* azobenzene (**1**) isomerization run over a time span of 30 minutes: (a) 48 μM azobenzene only (in the absence of AuNP), (b) 3.3 mM H_2O_2, (c) 33 μM Au^{3+} and (d) 33 μM HCl.[S3] Note no appreciable isomerization from the *cis* to *trans* stereoisomer can be observed in the absence of the AuNP catalyst. Control experiments were run in the presence of the aforementioned standards to ensure that any observable *cis-trans* isomerization was attributed to the presence of AuNP and not to due to the presence of any possible impurities remaining from the nanoparticle synthesis, including peroxide, ionic gold or acid from the acidic gold precursor.

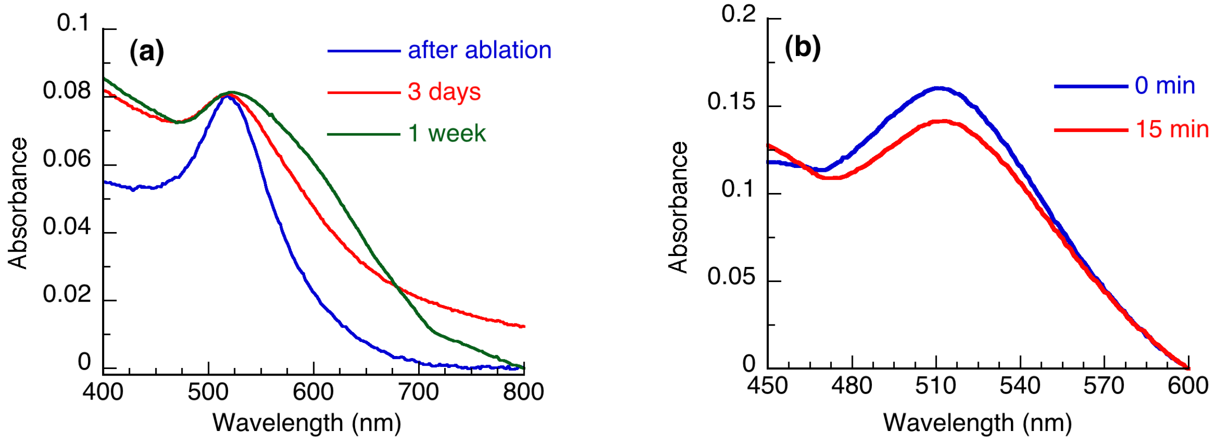

Figure S4. (a) UV-visible spectra of ablated AuNP immediately following ablation, after 3 days and one week of aging. Note the broadening of the surface plasmon band absorption near 600 nm, indicative of AuNP aggregation. (b) UV-visible spectrum of ablated AuNP (1.92 nM) in the presence of azobenzene 1 (48 μM) after 15 minutes, with emphasis on the AuNP surface plasmon region. A larger concentration of AuNP was used to better distinguish the surface plasmon absorbance and to demonstrate the stability of the AuNP in the presence of azobenzene substrates (no absorbance shift indicative of AuNP aggregation).

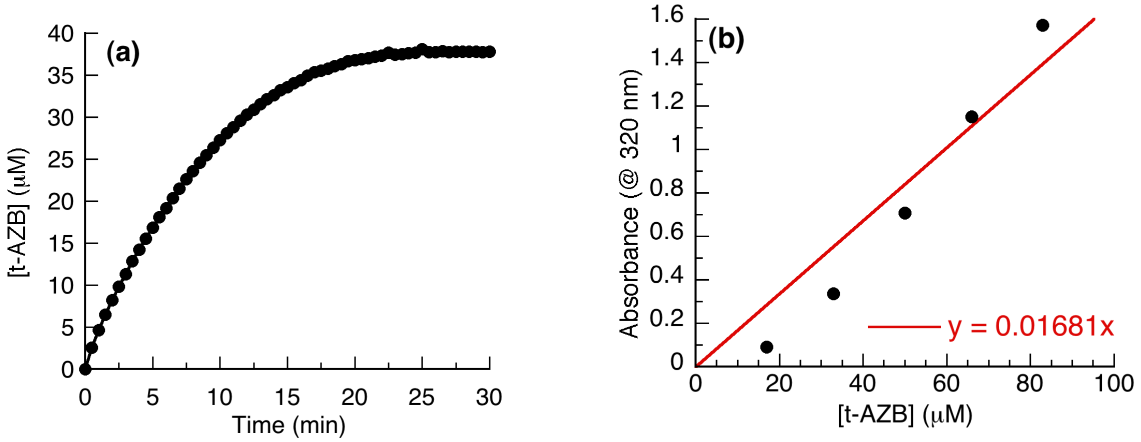

Figure S5. (a) Conversion rate growth curve and (b) the calibration curve (based on the Beer-Lambert Law) used to determine the extinction coefficients (in μM^{-1} cm^{-1}) the *trans* isomer of azobenzene **1** (t-AZB). Note an approximate conversion to 36 μM in the plateau region of the growth curve, as is discussed for Figures S6 and S7 (below).

Dependence on the concentration of AuNP

Exploratory experiments were carried out to examine the effect of AuNP concentration ([AuNP]) on the observed rate of catalytic *cis*-to-*trans* azobenzene conversion; this is illustrated in Figure S6. To our initial surprise, the upwards curvature of the plot seemed to suggest a cooperative effect. However, we believe that the observation can be explained simply by assuming that the *cis* isomer is far more soluble in water than the *trans* isomer, something for which there is precedent for other aromatic azo compounds,[S4] also reasonable in view of the larger dipole moment of the *cis* isomer; in fact, the solubility of *trans*-azobenzene in water is a mere 35 micromolar.

For the purpose of obtaining a qualitative understanding of how the stronger association of *trans*-azobenzene could influence the availability of free catalytic sites, we assumed that a 12 nm AuNP would have ~400 sites (equivalent to 38 $Å^2$ per molecule), and that all sites will act independently; thus the association equilibrium is given by:

$$tA + \mathrm{AuNP_{sites}} \leftrightarrows [tA \rightarrow \mathrm{AuNP_{sites}}] \quad (2)$$

where tA represents trans-azobenzene, and $\mathrm{AuNP_{sites}}$ the actual sites, equal in this example to 400 times the AuNP concentration. The association equilibrium constant is given by:

$$K_{eq} = \frac{[tA \rightarrow \mathrm{AuNP}_{sites}]}{[tA] \times [\mathrm{AuNP}_{sites}]} \quad (3)$$

We have assumed $K_{eq} = 500\ \mu M^{-1}$, and performed calculations for 0.2 μM *trans*-azobenzene, which is a small fraction of the typical ~36 μM total azobenzene concentration (see Figure S5), thus mimicking an early situation, or one where traces of the *trans* isomer are present at the start of the reaction, Figure S6. The selection of $K_{eq} = 500\ \mu M^{-1}$ simply reflects a practical visual search for K_{eq} values that led to curvature in the concentration region in which it is observed experimentally (see inset in Figure S7). Such visual approach does not provide a quantitative evaluation of the real value of K_{eq}, although it may be useful as a guide for the anticipated order of magnitude of this equilibrium constant.

From Figure S7 it is clear that non-linearity is to be expected when the reaction product has the ability to block access of the reactant to the catalytic sites; further, in the presence of a large excess of AuNP the concentration of available sites becomes a quasi-linear function of [AuNP], as expected.

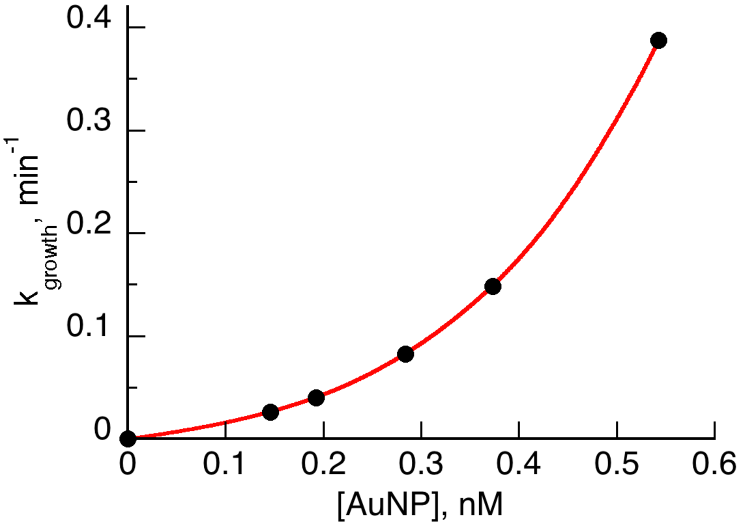

Figure S6. Dependence of *cis-trans* azobenzene **1** isomerization on AuNP catalyst concentration.

We emphasize that the plots of Figure S7 are meant to illustrate in a qualitative fashion that the non-linearity of Figure S6 is not surprising. A quantitative simulation would require values of K_{eq} for both isomers and inclusion in the calculation of the evolution of concentrations as the reaction proceeds as shown in Figures 1 and 2; further, a correction would be needed for any traces of *trans* azobenzene present initially.

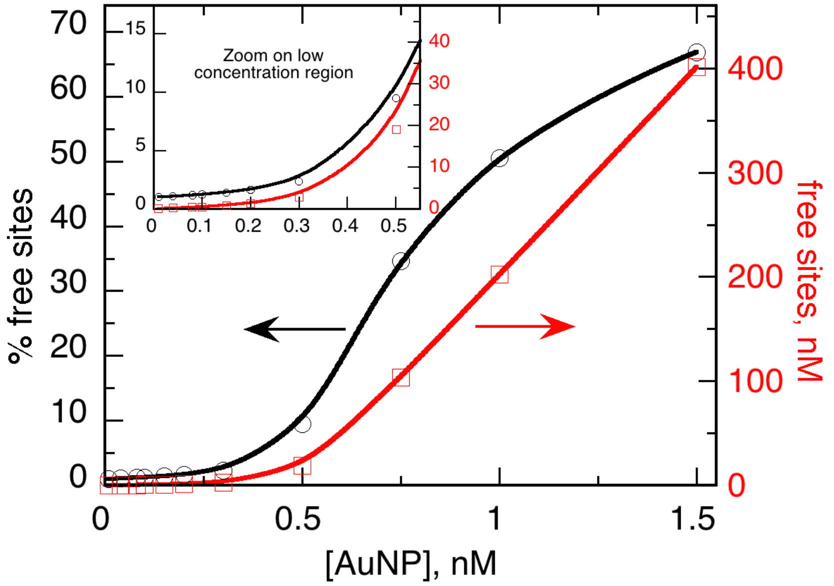

Figure S7. Availability of free catalytic sites as a function of the AuNP concentration, assuming that *trans*-azobenzene binds more strongly than *cis*-azobenzene. See text for details of assumptions. The calculation is meant to provide only qualitative guidance.

Table S1. Rate constant data for the AuNP (192 pM) mediated *cis-trans* isomerization of *para*-substituted azobenzenes with various batches of catalyst.

Batch	**Substrate**	k_{obs} **(min^{-1})**[a]	k_{rel}[b]
1	**1**	0.14 ± 0.03	1
	2	0.64 ± 0.02	4.5
	3	0.048 ± 0.01	0.3
2	**1**	0.33 ± 0.05	1
	4	0.17 ± 0.03	0.5
3	**1**	0.066 ± 0.006	1
	2	0.15 ± 0.04	2.3
	3	0.034 ± 0.001	0.5
	4	0.037 ± 0.009	0.6

[a] An average of two (batch 3) or three (batches 1 & 2) values obtained using the same batch of AuNP. Standard deviations were calculated at a 95% confidence level. [b] Relative rate constants for the *cis-trans* isomerization with respect to **1**.

From Table S1, it is evident that some batch-to-batch variability in the measured rate constants for *cis-trans* azobenzene isomerization can be expected, as has been previously cited.[S5,S6] However, and most importantly, the observed trend within the rate constant values remains consistent.

References:

(S1) McGilvray, K. L.; Granger, J.; Correia, M.; Banks, J. T.; Scaiano, J. C. *Phys. Chem. Chem. Phys.* **2011**, *13*, 11914.
(S2) Bueno Alejo, C. J.; D'Alfonso, C.; Pacioni, N. L.; González-Béjar, M.; Grenier, M.; Lanzalunga, O.; Alarcon, E. I.; Scaiano, J. C. *Langmuir* **2012**, *28*, 8183.
(S3) Ciccone, S.; Halpern, J. *Can. J. Chem.* **1959**, *37*, 1903.
(S4) Schanze, K. S.; Whitten, D. G. *J. Am. Chem. Soc.* **1983**, *105*, 6734.
(S5) Saha, K.; Agasti, S.S.; Kim, C., Li, X., Rotello, V.M. *Chem. Rev.* **2012**, *112*, 2739.
(S6) França, R.; Zhange, X.-F., Veres, T., Yahia, L'H., Sacher, E. *J. Coll. Interface Sci.* **2013**, *389*, 292.